Biomaterials 32 (2011) 4109–4117

Contents lists available at ScienceDirect

Biomaterials

journal homepage: www.elsevier.com/locate/biomaterials

The role of single cell derived vascular resident endothelial progenitor cells in the enhancement of vascularization in scaffold-based skin regeneration

Ziyang Zhang [a,**], Wulf D. Ito [b], Ursula Hopfner [a], Björn Böhmert [c], Mathias Kremer [d], Ann K. Reckhenrich [a], Yves Harder [a], Natalie Lund [e], Charli Kruse [c], Hans-Günther Machens [a], José T. Egaña [a,f,*]

[a] Department of Plastic Surgery and Hand Surgery, University Hospital Rechts der Isar, Faculty of Medicine, Technische Universität München, Munich, Germany
[b] Cardiovascular Center Oberallgaeu, Academic Teaching Hospital, University of Ulm, Immenstadt, Germany
[c] Fraunhofer Research Institute for Marine Biotechnology (EMB), Lübeck, Germany
[d] Department of Plastic Surgery and Hand Surgery, University of Lübeck, Lübeck, Germany
[e] Department of Experimental Cardiology, University Hospital Hamburg Eppendorf, Hamburg, Germany
[f] Center for Genome Regulation, Facultad de Ciencias, Universidad de Chile, Santiago, Chile

ARTICLE INFO

Article history:
Received 7 February 2011
Accepted 16 February 2011
Available online 23 March 2011

Keywords:
Tissue engineering
Tissue regeneration
Endothelial progenitor cells
Dermis
Vascularization

ABSTRACT

Increasing evidence suggests that vascular resident endothelial progenitor cells (VR-EPCs) are present in several organs, playing an important role in postnatal neovascularization. Here, we isolated and characterized VR-EPCs from cardiac tissue *in vitro*, evaluating their regenerative potential *in vivo*. VR-EPCs showed to be highly clonogenic and expressed several stem and differentiation markers. Under endothelial differentiation conditions, cells form capillary-like structures, in contrast to osteogenic or adipogenic differentiation conditions where no functional changes were observed. After seeding in scaffolds, cells were distributed homogeneously and directly attached to the scaffold. Then, cell seeded scaffolds were used to induce dermal regeneration in a nude mice full skin defect model. The presence of VR-EPCs enhanced dermal vascularization. Histological assays showed increased vessel number ($p < 0.05$) and cellularization ($p < 0.05$) in VR-EPCs group. In order to explore possible mechanisms of vascular regeneration, *in vitro* experiments were performed. Results showed that pro-angiogenic environments increased the migration capacity ($p < 0.001$) and ability to form capillary-like structures ($p < 0.05$) of VR-EPC. In addition, VR-EPCs secreted several pro-angiogenic molecules including VEGF and PDGF. These results indicate that a highly clonogenic population of VR-EPCs might be established *in vitro*, representing a new source for therapeutic vascularization in tissue engineering and regeneration.

1. Introduction

Dermal tissue regeneration is a complex process which involves several pathophysiological steps. Bioartificial scaffolds have been used for dermal tissue regeneration worldwide and represent the gold standard in some clinical conditions [1]. However, sub-optimal engraftment often leads to non-satisfying clinical results. One of the main reasons for this is the lack of vascularization within the scaffold. Thus, vascularization is considered a major challenge in tissue engineering and regeneration [1–4]. Oxygen, nutrients and other factors which are involved in the tissue regeneration process, can not reach to the wound area and so fail to trigger tissue regeneration, i.e. the development of newly formed micro-vessels. Thus, the enhancement of vascularization *in vivo* has been extensively studied. Among others, cell-based therapy has been proven to be promising. Evident vascularization was observed in a collagen scaffold containing fibroblasts for murine full skin regeneration after one week of implantation [5]. Further, bioengineered anterior cruciate ligament (bACL) was seeded with skin fibroblasts and vascularization was observed in all bACL with cells [6]. More recently, human mesenchymal stem cells have demonstrated to accelerate wound healing in patients with chronic non-healing wounds [7]. Our own studies have also shown that different glandular derived stem cells could also be used for enhancing dermal

* Corresponding author. Department of Plastic Surgery and Hand Surgery, University Hospital Rechts der Isar, Faculty of Medicine, Technische Universität München, Ismaningerstr. 22, 81675 Munich, Germany. Tel.: +49 89 4140 7510; fax: +49 89 4140 7515.
** Corresponding author. Department of Plastic Surgery and Hand Surgery, Klinikum rechts der Isar, Faculty of Medicine, Technische Universität München, Ismaningerstr. 22, 81675 Munich, Germany. Tel.: +49 89 4140 7510; fax: +49 89 4140 7515.
E-mail addresses: zhangziyang776@googlemail.com (Z. Zhang), tomasega@gmail.com (J.T. Egaña).

0142-9612/$ – see front matter © 2011 Elsevier Ltd. All rights reserved.
doi:10.1016/j.biomaterials.2011.02.036

scaffold vascularization via different mechanisms [1,2]. Although those results are promising, a current issue of debate with the use of stem cells is the possible side effect related to the un-controlled differentiation potential of stem cells *in vivo*. Thus, a possible way to overcome this problem is the use of endothelial progenitor cells (EPCs) because of the limited differentiation capacity of such cells.

EPCs are considered cells that can directly contribute to *in vivo* blood vessel formation. Since the discovery of adult endothelial progenitors in 1997 [8], numerous pre-clinical or clinical studies have been done using such cells for neovascularization. Recent studies showed that it is possible to isolate endothelial progenitors via single cell clonogenic assay [9–11]. In 2004, it was proven for the first time that a hierarchy of endothelial progenitors can be identified from umbilical cord blood [12] and adult vessel walls [13] via clonogenic assay. More recently, isolation of endothelial progenitors from the vascular endothelium has been discussed also in several other studies [14,15]. In this context, cardiac tissue has proven to be a rich source of different stem/progenitor cells [16]. Human cardiovascular progenitor cells which can differentiate into different lineages were found to derive from KDR positive stem cell population [17].

In the present study, we evaluated if vascular resident endothelial progenitor cells (VR-EPCs) isolated from rat cardiac vasculature tissue could be established based on their clonogenic and endothelial differentiation ability *in vitro*, and whether these cells could enhance dermal neovascularization *in vivo*.

2. Material and methods

2.1. Cell isolation and culture

Rat cardiac vascular resident cells were isolated as described before [18,19]. Briefly, rat heart vasculature was perfused *ex vivo* with Krebs-Ringer buffer containing 0.06% collagenase. Cells were then collected from the recirculation medium and grown under standard cell culture conditions using Dulbecco's Modified Eagle Medium (DMEM) supplemented with 10% Fetal Calf Serum (FCS) and antibiotics (penicillin and streptomycin). Confluent monolayer was split routinely 1:4 after washing with PBS and treatment with trypsin-EDTA. All reagents were purchased from Invitrogen (Karlsruhe, Germany). For clonal analysis, cells were cultured until reaching 80% confluence, detached and sorted by DAKO Cytomation MoFlo High Speed Cell Sorter (DAKO, Denmark). Next, a single cell was placed in a 96 well plate and cell growth was daily examined and counted. After 7 days, only the well with more cells was selected and subcultured for further studies.

2.2. Immunocytochemical analysis

Colonized cells were transferred into 2 well chamber slides (Becton Dickinson GmbH, Heidelberg, Germany) and cultured until sub-confluence. Then, cells were fixed for 10 min in 5% paraformaldehyde (PFA) containing 1 μg/ml 4',6-diamidino-2-phenylindole (DAPI; Roche Molecular Biochemicals, Mannheim, Germany) at room temperature and washed 3 times in phosphate buffered saline (PBS). Next, samples were blocked for 20 min in 1.65% normal goat serum at room temperature. Specimens were incubated with primary antibodies for 1 h at 37 °C in a humid chamber. Here we used antibodies against Nestin (mouse monoclonal, 1:250, Abcam, Cambridge, UK), Neurofilament (NF-H, rabbit polyclonal, 1:500, Serotec, Kidlington, UK), Troponin I Typ 1 (mouse monoclonal, 1:50, Acris, Herford, Germany), and GATA4 (mouse monoclonal, 1:100, Santa Cruz Biotechnology, Santa Cruz, USA). After rinsing 3 times with PBS, slides were incubated for 1 h at 37 °C with Cy3-labeled anti-mouse IgG (1:400) and FITC-labeled anti-rabbit IgG (1:200) (both purchase from Dianova, Hamburg, Germany). Then, slides were washed 3 times in PBS, covered in Vectashield mounting medium (Axxora, Grünberg, Germany) and analyzed with a fluorescence microscope (Axioskop Zeiss, Göttingen, Germany). Images were captured with the axiovision software (Zeiss, Göttingen, Germany) and fluorescence intensity was normalized to a black background. All immunocytochemical results showed typical morphologic features corresponding to targeted cellular structures, indicating a specific staining of these antibodies. The negative controls were carried out with the secondary antibodies alone and showed only unspecific faint staining (data not shown).

2.3. Real-time RT-PCR analysis

Total cellular RNA was isolated using the RNeasy Plus Mini Kit (Qiagen, Hilden, Germany) and a robotic workstation for the purification of RNA (QIAcube, Qiagen, Hilden, Germany). RNA concentration was determined by measuring the absorbance at 260 nm and 0.5 μg of total RNA was reverse transcribed into cDNA using QuantiTect reverse transcription kit (Qiagen, Hilden, Germany) according to the manufacturer's instructions. The quantitative real-time PCR (qRT-PCR) was performed with 1 μl cDNA in a 25 μl reaction volume using the QuantiTect SYBR Green PCR Kit and QuantiTect Primers (α-Actin: Rn_Acta2_1_SG, amplicon length: 82 bp; DMC1: GATA4: Rn_Gata4_1_SG, amplicon length: 70 bp; GFAP: Rn_Gfap_1_SG, amplicon length: 131 bp; Nestin: Rn_Nes_1_SG, amplicon length: 63 bp; Neurofilament L: RnNefl_1_SG, amplicon length: 69 bp; Oct-4: Rn_Pou5f_1_SG, amplicon length: 134; Troponin I Typ 1: Rn_Tnni1_1_SG, amplicon length: 137 bp: Von Willebrandt Factor: Rn_Vwf_1_SG, amplicon length: 107 bp (all Qiagen, Hilden, Germany). The amplification cycles were performed with the Mastercycler ep realplex (Eppendorf, Hamburg, Germany) and included a melting step (95 °C) and a combined annealing and amplification step (60 °C). All quantifications were performed in triplets. Automated gel electrophoresis was carried out with the QIAxcel capillary gel electrophoresis system (Qiagen, Hilden, Germany).

2.4. In vitro cell differentiation assay

For adipogenic or osteogenic differentiation, cells were cultured in differentiation medium containing adipogenic supplements (hMSC Differentiation BulletKit®—Adipogenic, Lonza, Cologne, Germany) or osteogenic supplements (hMSC Differentiation BulletKit®—Osteogenic, Lonza, Cologne, Germany) according to manufacture's instructions. Tube formation assay was performed as described before [1]. After differentiation, Oil red O staining (Invitrogen, Oregon, USA) and Von Kossa staining (Polysciences Europe GmbH, Eppelheim, Germany) were performed. Mouse pancreatic stem cells (PSC) were used as positive controls.

2.5. Scaffold for dermal regeneration and cell seeding

Integra matrix (IM) is a scaffold-based on bovine tendon collagen fibers cross linked with glycosaminoglycans which forms a porous biodegradable structure. On top, the collagen structure is covered with a removable silicon layer, which acts as a temporary epidermis. Pieces of IM (12 mm diameter) were dried with sterile gauze and placed in a 24 well plate, and then 300 μl of medium containing 1×10^6 cells were dropped over the scaffold being quickly absorbed for it. After 30 min of incubation, 1 ml of DMEM + 10% FCS was added into each well. Cell seeding efficiency was evaluated by removing the scaffold from the well and counting cells adhered to the culture dish. IM was kindly provided by Integra LifeScience Corporation, NJ, USA.

2.6. Cell visualization in the scaffold

After seeding for 14 days, Integra matrix containing cells was fixed in 3.7% paraformaldehyde (PFA, Sigma–Aldrich, Taufkirchen, Germany) for 30 min at room temperature (RT). Scaffolds were then permeabilized with 0.2% Triton for 30 min and stained for 1 h with TRITC-conjugated phalloidin (Sigma–Aldrich) at RT. Finally, samples were mounted in prolong anti-fade containing DAPI (Invitrogen, Oregon, USA) and analyzed by an FV10i confocal microscope (Olympus, Hamburg, Germany). For 3-dimensional view of the scaffold, slices from *Z*-axis were reconstructed by Amira 4.0 software (Visage Imaging GmbH, Berlin, Germany).

2.7. Quantification of metabolic activity in the scaffold

Cells (1×10^6) were seeded into each scaffold (12 mm of diameter) in 1 ml DMEM + 10% FCS. At days 1, 7 and 14 after seeding, medium was removed and scaffolds were incubated for 1 h in fresh medium containing 5 ng/ml MTT (Sigma–Aldrich, Taufkirchen, Germany). After incubation, medium was replaced by 500 μl dimethyl sulfoxide (DMSO; Sigma–Aldrich). In order to quantify metabolic activity, absorbance at 570 nm was measured in the DMSO containing soluble formazan blue. Scaffolds without cells were used as negative control.

2.8. Scaffold-based dermal regeneration model

Scaffolds obtained from 9 athymic nude mice (6–8 weeks old; Taconic, Copenhagen, Denmark) were analyzed. Animals were distributed in 2 groups: 4 controls (8 empty scaffolds, 2 scaffolds per animal) and 5 animals containing VR-EPCs (10 cell seeded scaffolds). Before transplantation, animals were anesthetized with ketamine (10 mg/kg) and xylazin (2.4 mg/kg) via intraperitoneal injection. Under general anesthesia, a bilateral full skin defect was created (10 mm diameter) in the back of the animals and the skin was replaced by control (empty) or cell seeded scaffolds (Fig. 4). In order to minimize possible artifacts during tissue harvesting, a titanized mesh (TIMESH, GfE Medizintechnik GmbH, Germany) was placed between the wound bed and scaffolds. Scaffolds were fixed to the wound by using non-absorbable sutures, and wounds were bandaged with sterile gauze. Two weeks after transplantation, animals were sacrificed by overdose of ketamine/xylazin and the scaffolds were removed for further analyses. All procedures *in vivo* were approved by the corresponding local ethical committees.

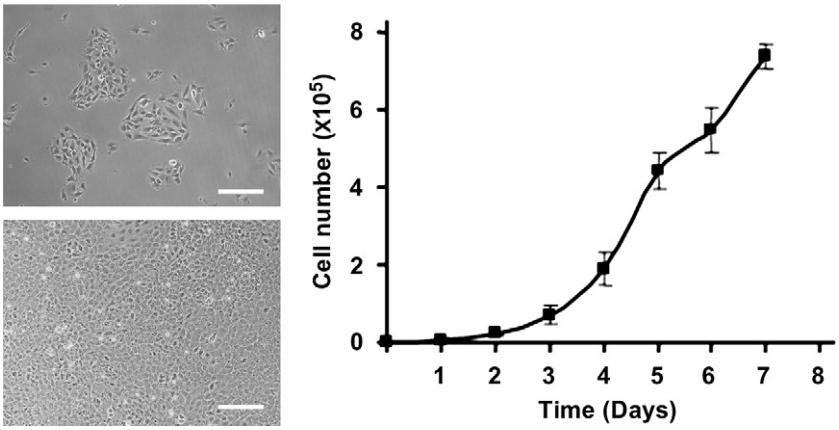

Fig. 1. Cell characterization. When cultured in DMEM supplemented with 10% FCS, VR-EPCs were strongly adherent to polycarbonate, showing a cobblestone like morphology (left) and high proliferation capacity (right). Scale bar represents 200 μm.

2.9. Scaffold vessel visualization and quantification

In order to quantify vascularization levels, tissue transillumination and digital segmentation were performed. After 2 weeks, skin from the back of the animals was removed and quickly placed over a transilluminator (Hama, LP 5000 K, Germany), digital pictures were obtained in TIF format (Olympus camera, C-5060, 5.1 Megapixels) and then processed for digital segmentation. Results were expressed as percentage of vascularization (vessel area and vessel length) compared to normal skin as described before [20]. The vessel analysis software used here can be downloaded at: http://www.isip.uni-luebeck.de/index.php?id=610.

2.10. Histological analysis

In order to analyze the density and distribution of cells and vessels in the implanted scaffolds, histological analyses were performed with hematoxylin and eosin (HE) and DAPI staining. Two weeks after implantation scaffolds were harvested, fixed with 3.7% PFA for 1 h, dehydrated, and embedded in paraffin. 10 μm thick paraffin sections were obtained from the center of the scaffold, deparaffinized and stained with standard HE and DAPI staining protocols. Functional blood vessels were identified by morphology and the presence of erythrocytes inside the vessel wall. Vessel number was obtained by counting on at least 3 different sections which were located at least 100 μm far of each other. Cellularization was evaluated in the border zone, defined by counting the cell number in 3 different areas (20× pictures) of each section in the cell infiltration zone which was defined by 0–240 μm (white dot line in Fig. 6B) above the border (red dot line in Fig. 6B) between the scaffold and the wound bed. All histological results were obtained by 2 independent researchers.

2.11. In vitro tube formation assay

VR-EPCs were cultured on polystyrene surface or Matrigel™ (BD Biosciences, USA) coated surfaces in DMEM + 10% FCS or in Endothelial Cell Growth Medium 2 (EGM) with supplement mix (PromoCell, Heidelberg, Germany). Matrigel was added into 48 well culture plates and allowed jellifying at 37 °C for 30 min. Next, 5×10^3 cells, in 0.5 ml medium, were added on top of the matrigel coated surface. After 1

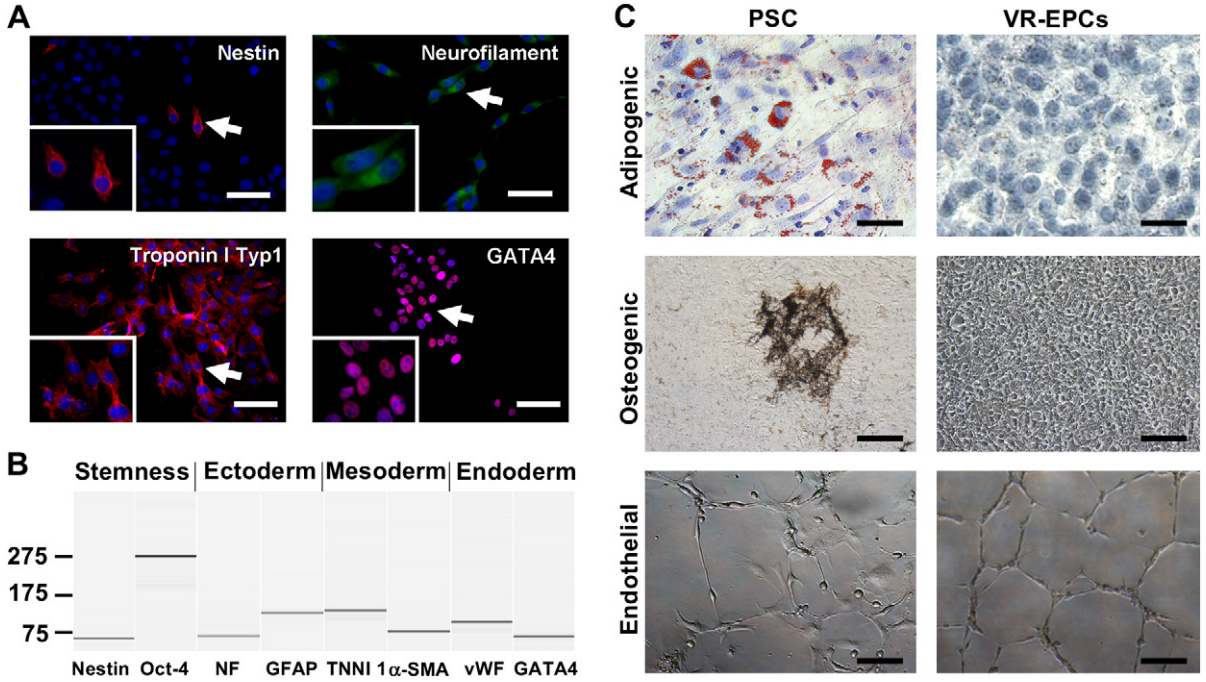

Fig. 2. Differentiation potential. At protein levels (A), VR-EPCs expressed stem (Nestin) and differentiation markers (Neurofilament (NF); Troponin I type 1 (TNNI 1) and GATA4. In addition, RT-PCR analysis (B) shows that VR-EPCs express the stem cells markers Nestin and Oct-4, and differentiation markers derived from the 3 different germ layers: Ectoderm (Glial Fibrilary Acidic Protein (GFAP) and NF), Mesoderm (Alpha Smooth Muscle Actin (α-SMA) and TNNI 1) and Endoderm (von Willebrandt factor (vWF) and GATA4). Cell plasticity was evaluated by seeding VR-EPCs under differentiation conditions (C). In contrast to pancreatic stem cells (PSC), no formations of fat vacuoles or calcium precipitate were found after seeding VR-EPCs in adipogenic or osteogenic differentiation medium. However, well defined capillary-like structures on matrigel coated surface were observed in both, PSC and VR-EPCs. Scale bar represents 100 μm in A, 50 μm in C upper panel and 200 μm in C middle and lower panel.

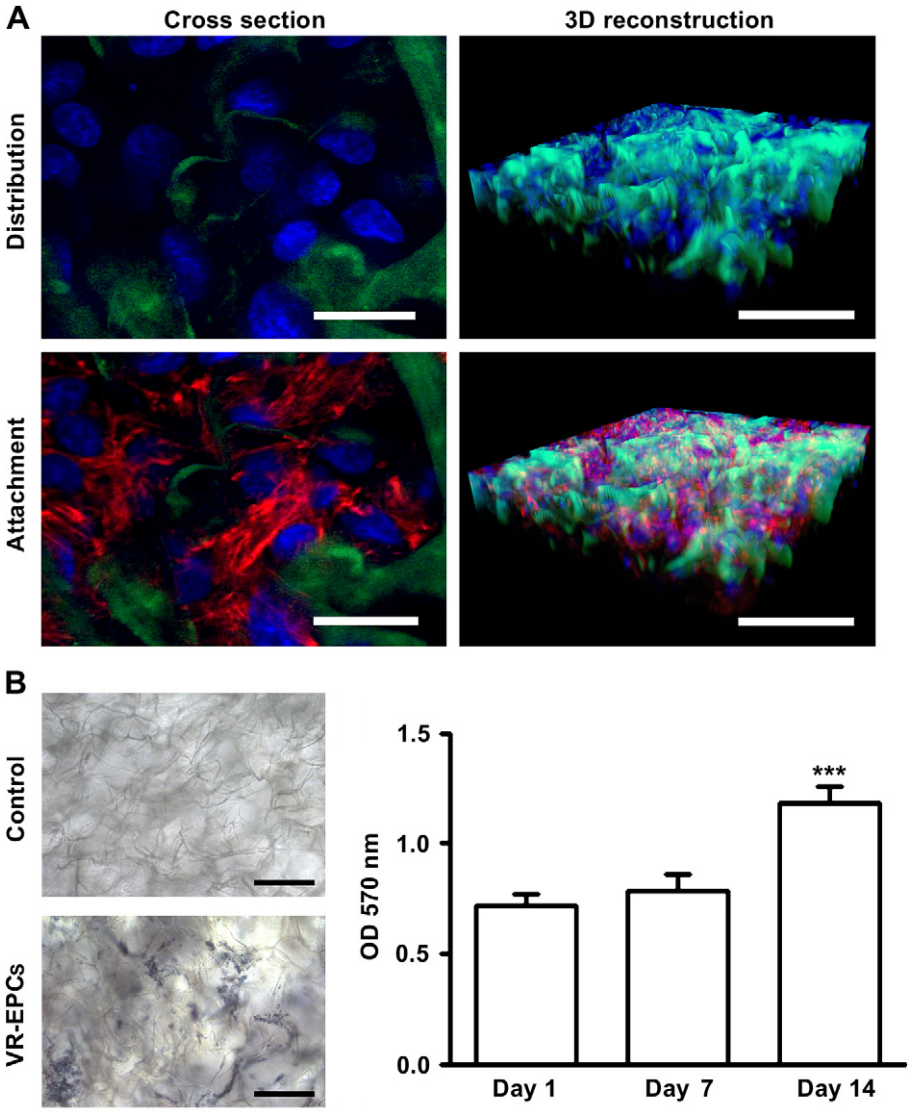

Fig. 3. Cell seeding in the scaffold. Distribution (DAPI/blue) and attachment (Phalloidin/red) of seeded cells to the scaffold (Autofluorescence/green) were evaluated (A). Left and right panels show a representative cross section and a 3-dimentional reconstruction of the scaffold containing cells respectively. After seeding, cell viability was evaluated by MTT assays (B). Left panel shows metabolically active cells (dark blue dots) in the scaffolds. Quantification of formazan blue formation showed a significant increase in metabolic activity on day 14 after seeding. (***$p < 0.001$) when compared to day 1 and day 7. Scale bar represents 20 μm in A left panel and, 100 μm in A right panel and in B. (For interpretation of the references to colour in this figure legend, the reader is referred to the web version of this article).

day, cells were fixed with 3.7% PFA and stained with TRITC-conjuncted Phalloidin (Sigma–Aldrich, Munich, Germany) and DAPI (Invitrogen, Oregon, USA). Quantification was evaluated by counting the number of tubes per field in 3 different random areas of each well.

2.12. In vitro cell migration assay

VR-EPCs (1×10^4) were seeded in a Culture-Insert (Ibidi, Martinsried, Germany) in 100 μl DMEM + 10% FCS. Once the cells reached confluence, the insert was removed and medium was replaced by fresh DMEM + 10% FCS or Endothelial Cell Growth Medium 2 (EGM; PromoCell, Germany). After 10 h, pictures were taken and cell migration in the open wound area (no cell covered area labeled in grey) was compared and quantified using TScratch as described before [21]. Results were obtained from 3 representative pictures of each well in 3 independent experiments and were expressed as the percentage of the open wound area at 10 h compared to time zero (0 h).

2.13. In vitro cytokine antibody profiling

VR-EPCs (5×10^6 cells) were seeded in 75 cm^2 culture flasks in DMEM + 10% FCS. After overnight incubation, medium was replaced for DMEM + 2% FCS and maintained in culture for another 72 h. Next, medium was collected and cytokine release was evaluated with a RayBio® Rat Cytokine Antibody Array 2 (RayBiotech, Georgia, USA) used according to manufacturer's instructions.

2.14. Statistical analysis

All analyses were performed in at least 3 independent experiments. Data are shown as mean ± SEM. Statistical comparisons between 2 groups were performed with two-tailed Student's *t*-test. Multiple comparisons between groups were applied when necessary with one way ANOVA followed by post hoc analysis. Differences among means were considered significant when $p < 0.05$.

3. Results

3.1. Cell characterization and differentiation

By selection for clonogenic cells, we were able to isolate a cell line which can be cultured for more than 100 passages. When seeded on polystyrene surfaces cells were adherent, showing a cobblestone like morphology (Fig. 1 left) and a high proliferation capacity, with a doubling time of about 18 h (Fig. 1 right). The expression of stem and differentiation markers was evaluated by immunocytochemistry and RT-PCR. Immunocytochemical analyses showed the expression of the stem cell marker nestin and differentiation

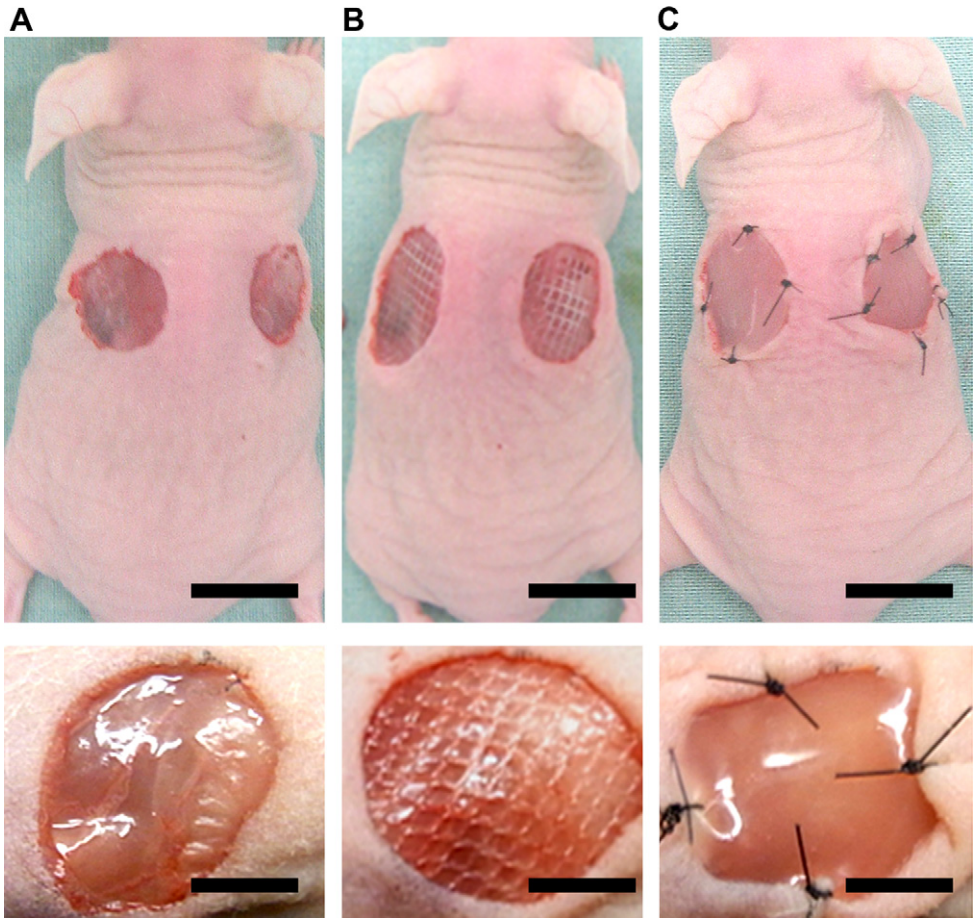

Fig. 4. Full skin dermal regeneration mouse model. A 10 mm diameter bilateral defect was created in the back of the animal (A). In order to minimize possible artifacts during the tissue harvesting, a titanized mesh was placed between the wound bed and the scaffold (B). Finally, the wound was covered with a scaffold for dermal regeneration (C). Scale bar represents 1 cm in the upper row and 0.5 cm in the lower.

markers from cells derived from the 3 different germal layers including: Neurofilament (ectodermal); Troponin I type 1 (mesodermal) and GATA4 (endodermal) (Fig. 2A). RNA expression analyses showed the stem cell markers (Nestin and Oct-4) and markers for multilineage differentiation including: Glial fibrilary acidic protein (GFAP); Neurofilament (NF); Troponin I type 1(TNNI 1); α-Smooth muscle actin (α-SMA); Von Willebrand factor (vWF) and GATA4 (Fig. 2B). After, we decided to evaluate the behavior of VR-EPCs when cultured under differentiation conditions [22]. First we evaluated the capacity of the cells for differentiating into adipocytes and osteoblasts after seeding under standard differentiation conditions. In contrast to pancreatic stem cells (PSC), the formation of fat vacuoles and the presence of calcium precipitates were not observed in VR-EPC. However both cell types, PSC and VR-EPCs, formed capillary-like structures on matrigel coated surfaces (Fig. 2C).

3.2. Cell seeding in the scaffold

Next, cells were seeded in a collagen scaffold and 2 weeks later confocal microscopic analysis was performed. A 3-dimensional reconstruction of the seeded scaffold showed that cells were distributed homogeneously, as observed by the presence of DNA staining (DAPI) in the whole structure (Fig. 3A upper panel). Additional staining for actin filaments (phalloidin) showed a direct interaction between the cells and the scaffold (Fig. 3A lower panel). In order to evaluate biocompatibility of the cells with scaffold, we performed MTT metabolic assays. Results showed that metabolically active cells were observed in the scaffold from day 1 (Fig. 3B left panel) being metabolically active for at least 2 weeks in culture (Fig. 3B right panel). A significant increase in metabolic activity was observed after 2 weeks in culture ($^{***}p < 0.001$), suggesting cell proliferation in the scaffold.

3.3. Tissue vascularization in vivo

In order to evaluate the capacity of the cells to increase vascularization *in vivo*, cell seeded or control (empty) scaffolds were engrafted in a bilateral full skin defect model (Fig. 4). The whole procedure was well tolerated for the animals. After 2 weeks, scaffolds were removed and analyzed by tissue transillumination and digital segmentation as described before [20]. We found that the presence of VR-EPCs significantly improved vascular regeneration. Quantification of vascularization showed improvements for both vessel area and length in the seeded scaffolds (Fig. 5; $^{***}p < 0.001$, $^{**}p < 0.01$). Afterward, vessel distribution and cellularization were evaluated by histological analyses. Results showed the presence of functional vessels in both, wound bed and scaffolds. Consistently with the results obtained by digital segmentation, a 6-fold increase in the vessel number was observed in cell seeded scaffolds (Fig. 6A; $^{*}p < 0.05$). After, cellularization of the scaffold at the border zone was analyzed. Results showed a significant increase in cell number at the area directly over the wound bed (Fig. 6B; $^{*}p < 0.05$).

3.4. Cell behavior under pro-angiogenic conditions

In order to determine the possible mechanisms involved in the vascular regeneration *in vivo* by VR-EPCs, here we analyzed cell

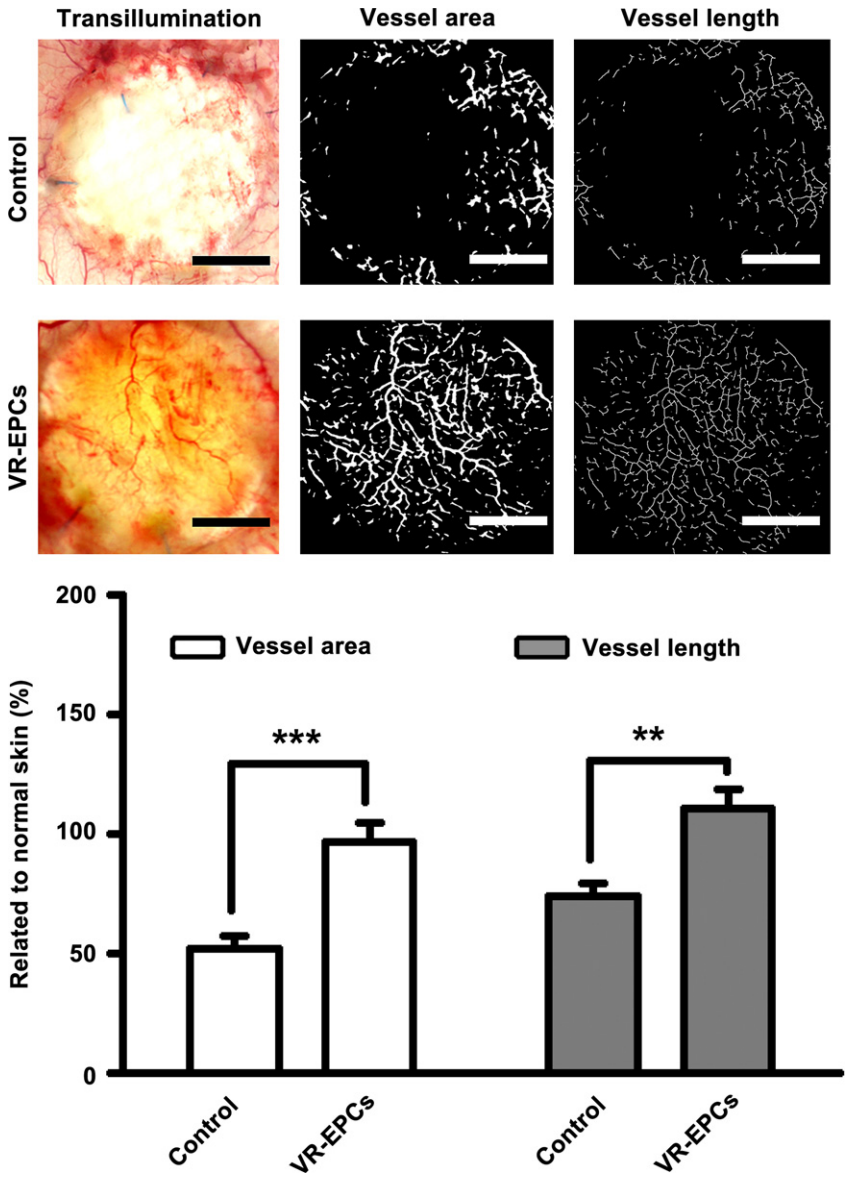

Fig. 5. Vascularization of the scaffold *in vivo*. Neovascularization of the scaffold was analyzed 2 weeks after transplantation. A representative scaffold of each group is shown by transillumination and digital segmentation (vessel area and vessel length). Quantification of the digital segmentation showed that seeded scaffolds (VR-EPCs; $n = 10$) were significantly more vascularized than controls (empty scaffolds; $n = 8$) in both, vessel area (***$p < 0.001$) and vessel length (**$p < 0.01$). Scale bar represents 3 mm.

behaviour under pro-angiogenic environments. After seeding cells on polystyrene surface, the presence of endothelial growth medium (EGM) induced the formation of capillary-like structures (Fig. 7A). The number of such structures was also found to be increased when cells were cultured on matrigel coated surfaces (Fig. 7B; *$p < 0.05$). In addition, cells responded to EGM by increasing their migration capacity evaluated by a scratch assay (Fig. 2D; ***$p < 0.001$). Interestingly, MTT assays showed that the presence of angiogenic factors decreased the metabolic activity of the cells (Fig. 7C; *$p < 0.05$).

3.5. Paracrine profile of VR-EPCs

It has been proven that stem/progenitor cells might contribute to neovascularization by releasing different soluble growth factors [23]. In order to determine whether VR-EPC can also contribute in this manner, we performed a cytokine antibody array. Here we have found that conditioned media contains chemoattractant (CXCL-1, MCP-1) and angiogenic (VEGF and PDGF-AA) molecules. Moreover, proteins related to tissue remodeling (TIMP-1, Activin-A and Agrin) were also detected (Fig. 8).

4. Discussion

The present study has demonstrated that highly clonogenic vascular resident endothelial progenitor cells (VR-EPCs) could be used to induce postnatal neovascularization in tissue engineering and regeneration. VR-EPCs showed several stem/progenitor cells features (Fig. 2) *in vitro* and might contribute in direct (Fig. 7) and/or paracrine manners (Fig. 8) to vascularization *in vivo* in a scaffold-based nude mice full skin defect model (Figs. 4–6).

Nowadays, there is a broad consensus that for most tissues and organs, vascularization is the key process for regeneration. Thus, autologous endothelial progenitor cells represent an attractive target cell source for therapeutic neovascularization. Since the discovery of endothelial progenitors in 1997, the definition and exact location of such cells have been under debate [11]. The

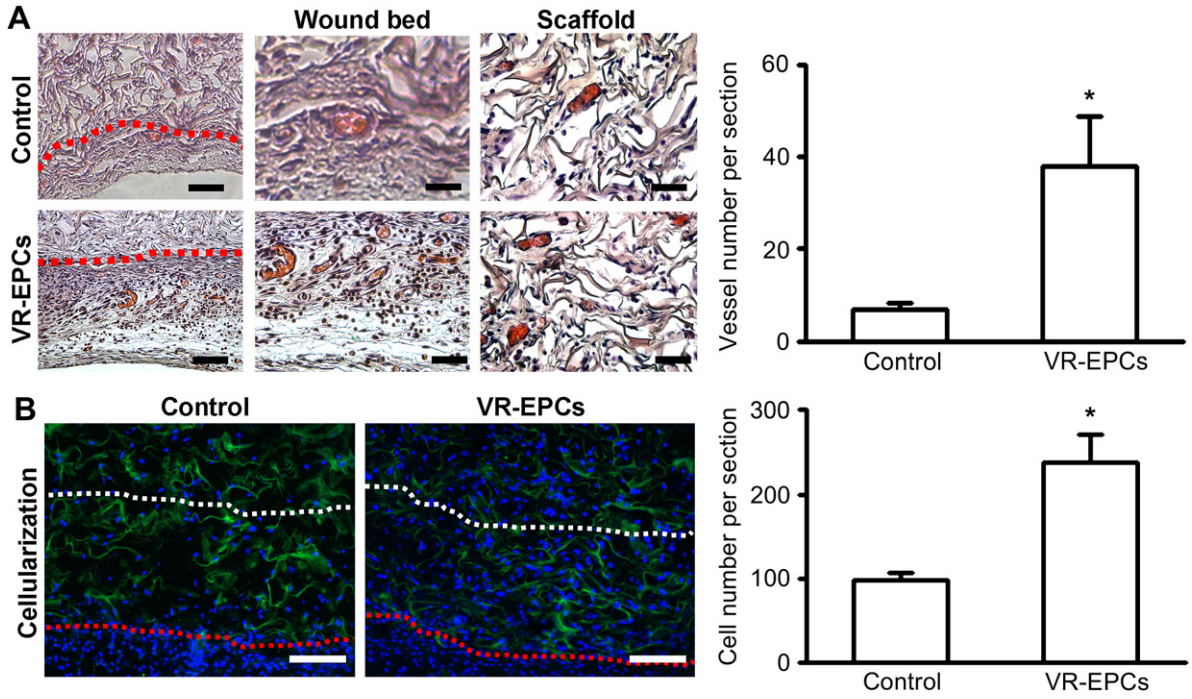

Fig. 6. Histological analysis. Sections of the scaffold showed that functional blood vessels were distributed in both, wound bed and scaffold, which are observed under and over the red dot line (A). Quantification of the number of blood vessels per section shows that the presence of VR-EPCs increased the vascularization levels ($*p < 0.05$). Cellularization of the scaffolds was quantified by counting the number of cells present at the border zone (between the red and white dot line). Results showed that in seeded scaffolds the number of cells was increased when compared to controls (B; $*p < 0.05$). Scale bar represents 200 μm in A (left panel) and B and, 50 μm in central and right panels in A.

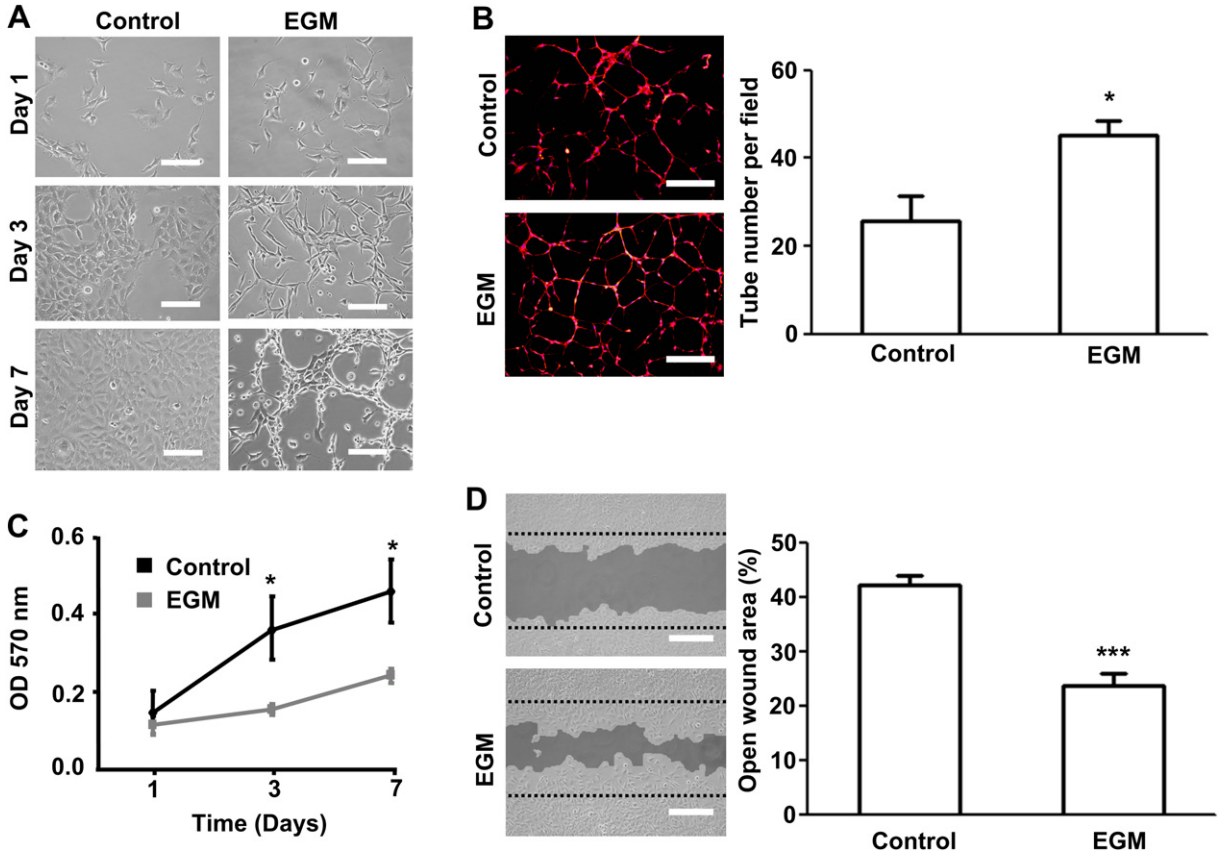

Fig. 7. Behavior of VR-EPCs in pro-angiogenic environments. Cells were cultured in control (DMEM + 10% FCS) or pro-angiogenic environments (Endothelial Growth Medium/EGM) and their behavior was compared. A dramatic change in morphology was observed when cultured in EGM (A). Moreover, EGM enhanced the ability of the cells to form capillary-like structures on matrigel coated surfaces (B), decrease metabolic activity (C) and, increased cell migration rate in a scratch assay (D). Scale bar represents 100 μm in A and, 200 μm in B and D. ($*p < 0.05$; $***p < 0.001$).

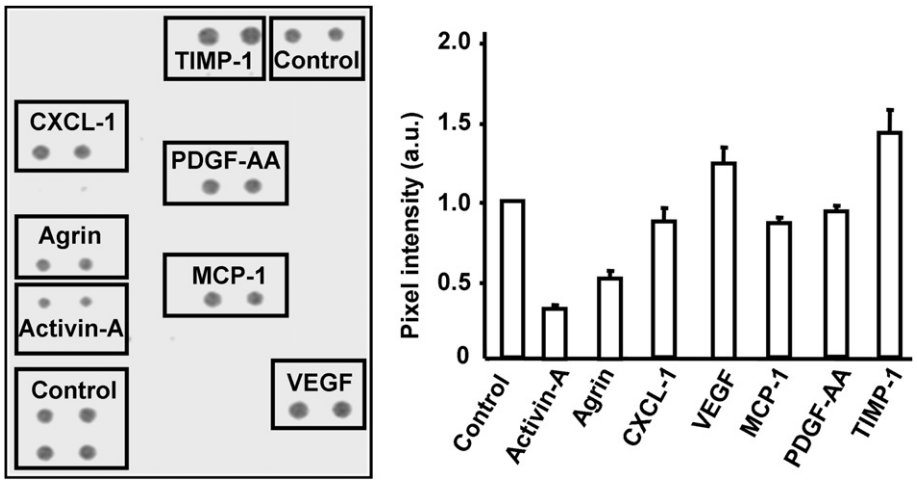

Fig. 8. Paracrine profile of VR-EPCs. The release of bioactive molecules from VR-EPCs was evaluated by cytokine protein array. After 3 days in culture, several bioactive molecules were found in the conditioned medium including: Agrin, Activin-A, CXCL-1, PDGF-AA, MCP-1, TIMP-1 and VEGF. Relative secretion was evaluated as pixel intensity related to the positive control.

current study presented 3 lines of evidences showing that our cells might represent a new type of EPCs. First, VR-EPCs obtained from a single cell clone have showed a highly clonogenic ability with a doubling time of approximately 18 h (Fig. 1). Although VR-EPCs were isolated from a single cell clone, they showed differentiation markers expressed in cells derived from all 3 different germ layers (Fig. 2A and B). Moreover, we also found nestin positive stem cell clones from the late outgrowth population (Fig. 2A). Second, compared to cells cultured under control condition (DMEM + 10% FCS), VR-EPCs cultured in endothelial cell growth medium showed a different phenotype (Fig. 7) including the formation of capillary-like structures on polystyrene and matrigel surface and the enhancement of cell migration ability. Furthermore, when seeded in scaffolds for *in vivo* dermal regeneration, VR-EPCs showed significant neovascularization ability compare to control *in vivo* (Figs. 5 and 6). Recently, several studies have suggested that the key elements for characterization of EPCs are the ability to form vascular structures in pro-angiogenic surfaces *in vitro* and the capacity to contribute to the postnatal neovascularization process *in vivo* [9,11,15,24,25]. According to this definition, the cells presented here correspond to EPCs. In addition, it is noteworthy that our cells share some similarities to late outgrowth endothelial cells (OECs) and endothelial colony forming cells (ECFCs). All these 3 groups of cells (OECs, ECFCs and VR-EPCs) exhibit cobblestone like morphology, own highly proliferative potential and form capillary-like structures on matrigel [10,11,15]. Indeed, here we have found that VR-EPCs form capillary-like structures even on uncoated polystyrene surface (Fig. 7A). Traditionally, EPCs can only form tube like structures on matrigel coated surface [26]. This new feature of the VR-EPCs may indicate an increased potential to develop microvessels compared to previously described EPCs.

Although here we show that endothelial environments increase both capillary-like structure formation and migration, yet the metabolic activity of the cells was significantly decreased when cultured in endothelial environment (Fig. 7C). This finding is in agreement with previous reports, showing that under differentiation conditions, proliferation was suppressed [27,28]. We also found nestin positive stem cells among the VR-EPCs. Although nestin is originally recognized as neural stem cell marker, several recent studies have shown the existence of nestin positive stem cells in rat cardiac tissue [29–31]. Furthermore, nestin positive stem cells have been described as a population that could contribute to the *de novo* vessel formation during myocardial infarction [31].

Although VR-EPCs might differentiate into different lineages *in vivo* since they have showed multilineage differentiation markers (Fig. 2), cells only responded to endothelial environment *in vitro* and we did not observe any side effects after the administration of our cells *in vivo*. This might be due to the fact that VR-EPCs preferentially differentiate into endothelial cells. However, further studies have to be performed to evaluate the differentiation potential of VR-EPCs *in vivo*. In addition to the possibility of direct contributions to the vessel formation, paracrine effects are also another possible explanation for the increase in vascularization observed *in vivo*. Stem/progenitor cells could induce vascularization also by secreting pro-angiogenic factors. It was demonstrated that EPCs released several pro-angiogenic factors which supported the ischemic tissue regeneration [23]. Bone marrow mononuclear cells improved cardiac function via both paracrine effects and direct differentiation [32]. In our study, we observed that VR-EPCs released cytokines related to angiogenesis and cytotaxis during *in vitro* culture (Fig. 8), VEGF and PDGF which are growth factors strongly related to angiogenesis are of special relevance. Previous studies have shown that hypoxia and PDGF increased VEGF expression in several cell types [33]. Since dermal scaffolds provide a hypoxic environment *in vitro* and *in vivo*, increased levels of angiogenic factors are expected to be released during the dermal regeneration process *in vivo*. The chemokines secreted by our cells (CXCL-1 and MCP-1) may be a possible mechanism for the better *in vivo* cellularization (Fig. 6B). However, the proliferation of our seeded cells inside the scaffold (Fig. 3) may also contribute to this. Additionally, MCP-1 which is a chemokine mainly involved in tissue injury and inflammation can directly induce angiogenesis via MCP-1-induced protein (MCPIP) [34] and also involved in arteriogenesis, which is a key process during tissue neovascularization [35].

5. Conclusions

The true nature of endothelial progenitor cells is still a matter of ongoing research. We report here that isolated vascular resident endothelial progenitor cells from rat cardiac tissue owning all three features that define newly discovered EPCs: 1) Highly clonogenic potential; 2) Tube formation ability; 3) Enhancing vascularization

in vivo. Our results indicate that VR-EPCs could be an alternative cell source to induce therapeutic neovascularization.

Acknowledgments

This work was supported by grants from University Hospital rechts der Isar, Technische Universität München To HGM; a clinic research grant from Technische Universität München to ZZ (KKF. No. 8744556); German Research Council (DFG) IT-13/1, IT- 13/2 and IT-13/3 to WDI; European Regional Development Fund (ERDF) to CK and FONDAP (Nr. 15090007) to JTE. Z.Z was supported by a scholarship from the China Scholarship Council. The authors gratefully acknowledge the support of the TUM's Thematic Graduate Center / Faculty Graduate Center Medical Life Science and Technology at Technische Universität München. The authors would like to thank Prof. Arndt Schilling for the critical revision of the manuscript, Prof. Ulrike Protzer and Miss Xiaoming Cheng for providing us the confocal microscopy. The authors declare no conflicts of interest.

References

[1] Egana JT, Danner S, Kremer M, Rapoport DH, Lohmeyer JA, Dye JF, et al. The use of glandular-derived stem cells to improve vascularization in scaffold-mediated dermal regeneration. Biomaterials 2009;30(30):5918–26.
[2] Salem H, Ciba P, Rapoport DH, Egana JT, Reithmayer K, Kadry M, et al. The influence of pancreas-derived stem cells on scaffold based skin regeneration. Biomaterials 2009;30(5):789–96.
[3] Egana JT, Fierro FA, Kruger S, Bornhauser M, Huss R, Lavandero S, et al. Use of human mesenchymal cells to improve vascularization in a mouse model for scaffold-based dermal regeneration. Tissue Eng Part A 2009;15(5):1191–200.
[4] Liu S, Zhang H, Zhang X, Lu W, Huang X, Xie H, et al. Synergistic angiogenesis promoting effects of extracellular matrix scaffolds and adipose-derived stem cells during wound repair. Tissue Eng Part A; 2010 [Epub ahead of print].
[5] Su QH, Yang MJ, Zhou HM. Repair of murine full skin loss with composite skin of collagen scaffold containing living cells. Zhonghua Shao Shang Za Zhi 2003;19(6):358–60.
[6] Tremblay P, Cloutier R, Lamontagne J, Belzil AM, Larkin AM, Chouinard L, et al. Potential of skin fibroblasts for application to anterior cruciate ligament tissue engineering. Cell Transplant; 2010 [Epub ahead of print].
[7] Falanga V, Iwamoto S, Chartier M, Yufit T, Butmarc J, Kouttab N, et al. Autologous bone marrow-derived cultured mesenchymal stem cells delivered in a fibrin spray accelerate healing in murine and human cutaneous wounds. Tissue Eng 2007;13(6):1299–312.
[8] Asahara T, Murohara T, Sullivan A, Silver M, van der Zee R, Li T, et al. Isolation of putative progenitor endothelial cells for angiogenesis. Science 1997;275 (5302):964–7.
[9] Timmermans F, Plum J, Yoder MC, Ingram DA, Vandekerckhove B, Case J. Endothelial progenitor cells: identity defined? J Cell Mol Med 2009;13 (1):87–102.
[10] Richardson MR, Yoder MC. Endothelial progenitor cells: quo vadis? J Mol Cell Cardiol 2011;50(2):266–72.
[11] Yoder MC, Mead LE, Prater D, Krier TR, Mroueh KN, Li F, et al. Redefining endothelial progenitor cells via clonal analysis and hematopoietic stem/progenitor cell principals. Blood 2007;109(5):1801–9.
[12] Ingram DA, Mead LE, Tanaka H, Meade V, Fenoglio A, Mortell K, et al. Identification of a novel hierarchy of endothelial progenitor cells using human peripheral and umbilical cord blood. Blood 2004;104(9):2752–60.
[13] Ingram DA, Mead LE, Moore DB, Woodard W, Fenoglio A, Yoder MC. Vessel wall-derived endothelial cells rapidly proliferate because they contain a complete hierarchy of endothelial progenitor cells. Blood 2005;105 (7):2783–6.
[14] Yoder MC. Is endothelium the origin of endothelial progenitor cells? Arterioscler Thromb Vasc Biol 2010;30(6):1094–103.
[15] Watt SM, Athanassopoulos A, Harris AL, Tsaknakis G. Human endothelial stem/progenitor cells, angiogenic factors and vascular repair. J R Soc Interface 2010;7(Suppl. 6):S731–51.
[16] Messina E, De Angelis L, Frati G, Morrone S, Chimenti S, Fiordaliso F, et al. Isolation and expansion of adult cardiac stem cells from human and murine heart. Circ Res 2004;95(9):911–21.
[17] Yang L, Soonpaa MH, Adler ED, Roepke TK, Kattman SJ, Kennedy M, et al. Human cardiovascular progenitor cells develop from a KDR + embryonic-stem-cell-derived population. Nature 2008;453(7194):524–8.
[18] Linssen MC, Engels W, Lemmens PJ, Heijnen VV, Van Bilsen M, Reneman RS, et al. Production of arachidonic acid metabolites in adult rat cardiac myocytes, endothelial cells, and fibroblast-like cells. Am J Phys 1993;264(3 Pt 2):H973–82.
[19] Derhaag JG, Duijvestijn AM, Emeis JJ, Engels W, van Breda Vriesman PJ. Production and characterization of spontaneous rat heart endothelial cell lines. Lab Invest 1996;74(2):437–51.
[20] Egana JT, Condurache A, Lohmeyer JA, Kremer M, Stockelhuber BM, Lavandero S, et al. Ex vivo method to visualize and quantify vascular networks in native and tissue engineered skin. Langenbecks Arch Surg 2009;394 (2):349–56.
[21] Geback T, Schulz MM, Koumoutsakos P, Detmar M. TScratch: a novel and simple software tool for automated analysis of monolayer wound healing assays. Biotechniques 2009;46(4):265–74.
[22] Tashiro K, Inamura M, Kawabata K, Sakurai F, Yamanishi K, Hayakawa T, et al. Efficient adipocyte and osteoblast differentiation from mouse induced pluripotent stem cells by adenoviral transduction. Stem Cells 2009;27 (8):1802–11.
[23] Urbich C, Aicher A, Heeschen C, Dernbach E, Hofmann WK, Zeiher AM, et al. Soluble factors released by endothelial progenitor cells promote migration of endothelial cells and cardiac resident progenitor cells. J Mol Cell Cardiol 2005;39(5):733–42.
[24] Yao H, Liu B, Wang X, Lan Y, Hou N, Yang X, et al. Identification of high proliferative potential precursors with hemangioblastic activity in the mouse aorta-gonad- mesonephros region. Stem Cells 2007;25(6):1423–30.
[25] Hirschi KK, Ingram DA, Yoder MC. Assessing identity, phenotype, and fate of endothelial progenitor cells. Arterioscler Thromb Vasc Biol 2008;28 (9):1584–95.
[26] Kleinman HK, Martin GR. Matrigel: basement membrane matrix with biological activity. Semin Cancer Biol 2005;15(5):378–86.
[27] Xia K, Xue H, Dong D, Zhu S, Wang J, Zhang Q, et al. Identification of the proliferation/differentiation switch in the cellular network of multicellular organisms. PLoS Comput Biol 2006;2(11):e145.
[28] Brown G, Hughes PJ, Michell RH. Cell differentiation and proliferation–simultaneous but independent? Exp Cell Res 2003;291(2):282–8.
[29] Beguin PC, El-Helou V, Assimakopoulos J, Clement R, Gosselin H, Brugada R, et al. The phenotype and potential origin of nestin + cardiac myocyte-like cells following infarction. J Appl Phys 2009;107(4):1241–8.
[30] El-Helou V, Dupuis J, Proulx C, Drapeau J, Clement R, Gosselin H, et al. Resident nestin + neural-like cells and fibers are detected in normal and damaged rat myocardium. Hypertension 2005;46(5):1219–25.
[31] Hoffman RM. The potential of nestin-expressing hair follicle stem cells in regenerative medicine. Expert Opin Biol Ther 2007;7(3):289–91.
[32] Yoon CH, Koyanagi M, Iekushi K, Seeger F, Urbich C, Zeiher AM, et al. Mechanism of improved cardiac function after bone marrow mononuclear cell therapy: role of cardiovascular lineage commitment. Circulation 2010;121 (18):2001–11.
[33] Petersen W, Pufe T, Zantop T, Tillmann B, Mentlein R. Hypoxia and PDGF have a synergistic effect that increases the expression of the angiogenetic peptide vascular endothelial growth factor in achilles tendon fibroblasts. Arch Orthop Trauma Surg 2003;123(9):485–8.
[34] Niu J, Azfer A, Zhelyabovska O, Fatma S, Kolattukudy PE. Monocyte chemotactic protein (MCP)-1 promotes angiogenesis via a novel transcription factor, MCP-1-induced protein (MCPIP). J Biol Chem 2008;283(21):14542–51.
[35] Ito WD, Arras M, Winkler B, Scholz D, Schaper J, Schaper W. Monocyte chemotactic protein-1 increases collateral and peripheral conductance after femoral artery occlusion. Circ Res 1997;80(6):829–37.